Supporting Information

Exponentially enhanced photocatalytic alkane production from biomass-derived fatty acid decarboxylation via self-heating induced conformational inversion

Qiang Huang[1,4#], Chunlin Hao[2#], Guibao Guo[3*], Hongwei Ji[1,4], Shengli An[2*], Wanhong Ma[1,4*], and Jincai Zhao[1,4]

[1]Key Laboratory of Photochemistry, CAS Research/Education Center for Excellence in Molecular Sciences, Institute of Chemistry Chinese Academy of Sciences, Beijing 100190, P. R. China

[2]Inner Mongolia Key Laboratory of Advanced Ceramic Materials and Devices, Inner Mongolia University of Science and Technology; Baotou 014010, P. R. China.

[3]School of Chemistry and Chemical Engineering, Inner Mongolia University of Science & Technology; Baotou 014010, P. R. China.

[4]University of Chinese Academy of Sciences; Beijing, 100049, P. R. China

*Corresponding author: Guibao Guo (Email: ggb66733@sohu.com), Shengli An (Email: san@imust.edu.cn), Wanhong Ma (whma@iccas.ac.cn)

#These authors contributed equally.

Table of Contents

Experimental Procedures

Chemicals

P25 (commercial TiO_2, >99%), stearic acid (97%), behenic acid (>99%), heneicosanoic acid (>98%), arachidic acid (98%), nonadecanoic acid (98+%), heptadecanoic acid (99%), palmitic acid (98%), myristic acid (99%), tridecanoic acid (>98%), lauric acid (99%) sodium stearate (>97.0%), deuterium chloride (for NMR, 1M solution in D_2O, 99.8 atom% D), D_2O (for NMR, 99.9 atom%), 1-dodecanol (>99%) and brominated diphenyl ether (99%) were purchased from Beijing Innochem Science & Technology Co., Ltd, China. Benzotrifluoride (99%), amylbenzene (>98%), dimethyl sulfoxide (>99%), 1-Methyl-2-pyrrolidone (>99%), butyl ether ($\geq$99.5%), n-propylbenzene (98%), hexyl ether (>98%), acetonitrile ($\geq$99.9%), n-octadecane (99%), n-hexadecane (>98%), n-nonadecane (99%), n-pentadecane (99%), n-tetradecane (99%), n-tridecane (99%), n-dodecane (99%), n-undecane (>99%), decane (>99%) and other alkanes were purchased from Shanghai Aladdin Bio-Chem Technology Co. All the above chemicals and catalysts were used as received without further purification.

Photocatalytic reaction

Photocatalytic decarboxylation reactions were conducted at ambient pressure in an N_2 atmosphere under LED (768 W, 410 nm) irradiation without an external heat supply. Typically, 25ml of the reaction solution was prepared by 125 mg of TiO_2, fatty acid (0.05 M), n-octadecane (internal standard, 0.05 M) and n-tetradecane (solvent). The reaction solution was placed in a reactor filled with N_2 and exposed to light under stirring. A condensing unit keeps the vaporized reaction solution returning to the liquid phase. The reaction solution that finished the photocatalytic reaction was subjected to an esterification reaction with an equal volume of methanol catalyzed by concentrated sulfuric acid at 85 °C. Finally, the reaction solution of the completed esterification reaction was separated by centrifugation and the supernatant was taken for GC quantitative analysis. This method was used for all quantitative analyses.

The quantitative method for product analysis

The products of light-driven decarboxylation of fatty acids were quantified by gas chromatography (GC, Agilent 7820A), which is equipped with a flame ionization detector (FID) and with a 30 m×320 μm×0.25 μm HP-5 capillary column. The injector and detector temperatures were 270 °C and 280 °C, respectively. The oven temperature was programmed as 4 min soak at 40 °C followed by a 10 °C/min ramp up to 270 °C, which was held for 15 min. The products in the liquid phase were identified by gas chromatography-mass spectrometry (GC-MS, Agilent 7890B/7000C) equipped with a 30 m×250 μm×0.25 μm HP-5MS capillary column and flame ionization detector (FID). The temperature of the injector and detector were 270 °C and 300°C, respectively. The following temperature program was used for analysis: 40 °C (10 °C/min) hold for 4 min and 320 °C (10 °C/min) hold for 15 min. The establishment of an internal standard method standard curve is a more accurate method for quantitative analysis in gas chromatography. Here we used stearic acid as an example to establish a standard curve, and other fatty acids are similar to it. Take stearic acid, the internal standard curve method was established as follows, 5.0894 g (0.02 mol) of n-octadecane was dissolved in n-tetradecane (solvent) to make 100 mL, shaking for 30 min to obtain 0.2 mol/L of internal standard solution. Five volumetric flasks of 10 mL were marked with 1 to 5, which were accurately added to 2.5 mL of n-octadecane internal standard solution. The stearic acid of 0.01 mol/L, 0.02 mol/L, 0.03 mol/L, 0.04 mol/L and 0.05 mol/L was put into the 10 mL volumetric flask labeled with the serial numbers 1, 2, 3, 4 and 5, respectively, and the same concentration of n-heptadecane as stearic acid was added to the above 10 mL volumetric flask. Then each volumetric flask was fixed with n-tetradecane, and shaken with ultrasound for 30 min. The mixture

in the volumetric flask was reacted with 10 mL of methanol and 1 ml of concentrated sulfuric acid in a round bottom flask at 85 °C for 2 h. The mixture of the completed esterification reaction was separated by centrifugation and the supernatant was taken for GC analysis (Agilent 7820A). The corresponding peak area of each substance was obtained by gas chromatography. In this process, n-octadecane is used as an internal standard. The concentrations of n-heptadecane and n-octadecane are known, and the ratio of n-heptadecane to n-octadecane is taken as the abscissa. Taking the ratio of the peak area of n-heptadecane to n-octadecane as the ordinate, the standard curve equation of n-heptadecane can be obtained by linear fitting, $Y=0.8795X+0.00292$ ($R^2=0.9997$). Similarly, taking the ratio of stearic acid concentration to n-octadecane concentration as the abscissa, and the ratio of the peak area of methyl stearate to n-octadecane as the ordinate, a standard curve equation of the surplus of stearic acid can be obtained, $Y=0.94745X+0.00343$ ($R^2=0.9993$).

The yield of n-heptadecane, the surplus of stearic acid, and the selectivity of n-heptadecane can be calculated by Equation S1~S3.

$$\text{Yield (\%)} = \frac{A_{17}/A_{18} - 0.00292}{0.8795} \times 100\% \tag{S1}$$

$$\text{Surplus (\%)} = \frac{A_0/A_{18} - 0.00343}{0.94745} \times 100\% \tag{S2}$$

$$\text{Selectivity (\%)} = \frac{\text{Yield (\%)}}{1 - \text{Surplus (\%)}} \times 100\% \tag{S3}$$

Where A_{17} is the peak area of n-heptadecane; A_{18} is the peak area of n-octadecane (internal standard); A_0 is the peak area of methyl stearate.

Preparation of $CH_3(CH_2)_{16}CO_2D$

Sodium stearate (>97.0%, TCL) and excessive deuterium chloride (1 M solution in D_2O, 99.8 atom% D, ACROS) were added into a stand-up flask (250 mL) under continuous magnetic stirring in 80 °C silicone oil pan for 6 h. After the reaction was completed, it was cooled to room temperature. The solid sample was extracted and washed 3 times with D_2O (for NMR, 99.9 atom%) to remove sodium chloride. Finally, the obtained products were dried in a glass dryer with a discolouring desiccant. The final products were detected by mass spectrometry (TOF MS EI$^+$).

Free-radical intermediates trapping experiments

Radical-trapping reactions: The reactant mixture consisted of stearic acid (0.05 M), TiO_2 catalyst (125 mg), TEMPO (0.3 M) and n-nonane solvent (24 mL). After being filled with N_2, the reaction cell was irradiated by LED (410 nm, 10.25 W/cm^2) with continuous stirring (300 r.p.m) with continuous water cooling. After reacting for 30 min, the mixture was analyzed by gas chromatography (GC, Agilent 7820A; GC/MS, Agilent 7890B, Agilent 7000C).

Isotope experiments

The isotope experiment was carried out at normal pressure under LED (410 nm, 10.25W/cm^2) illumination with continuous stirring with continuous water cooling. The reactant mixture (25 mL) consisted of TiO_2 catalyst (125 mg), $CH_3(CH_2)_{16}CO_2D$ (3.5558 g) and n-tetradecane solvent. Before irradiation, the system was filled with nitrogen for 90 min to remove the dissolved oxygen. After

reacting for 6 h, the reaction mixture was purified by silica gel column chromatography to remove the TiO_2 catalyst and unreacted stearic acid. Then, the obtained n-alkane mixture was further purified by vacuum distillation to obtain the target C_{n-1} n-alkane. The obtained C_{n-1} n-alkane was detected by mass spectrometry (TOF MS EI[+])

General characterization

The in-situ DRIFT spectra were collected on a Bruker VERTEX 70v instrument. The sample was prepared by mixing stearic acid (20 mg) and TiO_2 (100 mg) by grinding them sufficiently. The sample was pressed to fill the alumina crucible (6 mm diameter) and the exposed surface of the sample (the surface that receives light) is flat. The sample compartment is purged with a continuous stream of Ar gas to eliminate interference from CO_2.

The in situ ESR spectra were collected on a Bruker E500 spectrometer with a field modulation of 100 kHz. The microwave frequency was maintained at 9.4 GHz. The powder samples consisted of a well-ground mixture of stearic acid (20 mg) and TiO_2 (100 mg). 10 mg of the sample was placed in a paramagnetic tube and placed in an Ar glove box to replace the air.

The in situ XPS spectra were collected on an AXIS SUPRA+ spectrometer, using monochromatic Al Kα X-ray as a light source. The powder samples consisted of a well-ground mixture of stearic acid (20 mg) and TiO_2 (100 mg). The prepared powder sample was pressed into a sheet at 4~5 MPa.

X-ray diffraction analyses were collected on a D8 ADVANCE diffractometer, using Cu-Kα radiation. The data were recorded over a 2θ range of 10 ~ 85°.

UV-Vis absorption spectra were collected from a UV3101PC spectrophotometer. The scanning range was 200~800 nm, and the scanning speed was 600 nm/min.

^{1}H and ^{13}C NMR spectra were collected on a Bruker Avance III 400 MHz spectrometer at room temperature.

The Brunauer-Emmett-Teller (BET) specific surface area of the prepared sample was determined by nitrogen adsorption in an Autosorb-iQ.

Determination of apparent quantum efficiency (AQE)

The AQE of visible-light-driven decarboxylation of fatty acids was determined over TiO_2 by potassium ferrioxalate actinometer with LED (total power 768 W, intensity 10.25W/cm^{2} at 410 nm wavelength) by bottom illumination. The AQE (%) was calculated according to Equation S4 and the previous report[1].

$$\Phi_c = \frac{k_c \Phi_a}{2.303 k_a \varepsilon_{410} L} \times 100\%$$

(S4)

Where Φ_c is the AQE of n-alkane formation, k_c is the rate constant (min^{-1}) of visible-light-driven fatty acid decarboxylation, Φ_a is the photolysis quantum yield of $K_3Fe(C_2O_4)_3$ at 410 nm is about 1.14[2], k_a is the rate constant (min^{-1}) of $K_3Fe(C_2O_4)_3$ under LED (768 W, 410 nm) illumination, ε_{410} is the molar absorption coefficient of TiO_2 catalyst at 410 nm and L is the effective optical path of quartz reactor. The detailed calculation process is as follows:

Determination of reaction rate constant of photocatalytic stearic acid decarboxylation. Generally, 125 mg TiO_2 catalyst was dispersed uniformly in a 25 mL mixed solution of 0.05 M stearic acid, 0.05 M octadecane and a kind of n-alkanes solvent (C6 n-hexane to C14 n-tetradecane) in a quartz reactor. After being filled with N_2, the reaction cell was irradiated by LED (410 nm, 10.25 W/cm^2) with continuous stirring (300 r.p.m) with continuous water cooling for the desired reaction time. After the reaction finished, 25 mL of methanol and 2.5 mL of concentrated sulfuric acid were added and the mixture was heated at 85 °C for 2 h for esterification. Finally, the reaction mixture was centrifuged for GC analysis.

Determination of photolysis rate constant of $K_3Fe(C_2O_4)_3$. 25 mL of 4.079×10^{-3} mol/L $K_3Fe(C_2O_4)_3$ was filled into the quartz reactor. The reactor was then irradiated by LED (410 nm, 10.25 W/cm^2) in a cooled circulating water system under stirring (300 r.p.m). The samples were taken at 4, 6, 8, 10, 12 and 14 min respectively, and the absorbance was measured by UV/vis spectrophotometer. The concentration was obtained according to Lambert's law to determine the reaction rate constant.

Determination of molar absorption coefficient of Fe^{2+} (ε_{510}). The buffer solution was obtained by adding 600 mL of 1.0 mol/L sodium acetate solution, 300 mL of 0.5 mol/L sulfuric acid solution, and diluted to 1 L with deionized water. Take 0.5, 1, 2, 3, 4, 6, 8 and 10 mL of 5.0×10^{-4} mol/L $FeSO_4$ solution, into 50 mL volumetric flasks respectively. Then each sample was added with 2 mL of 1.0 mol/L sulfuric acid, 10 mL acetate buffer, 4 mL of 0.1 % aqueous 1,10-phenanthroline solution in turn, and then was diluted to 50 mL with deionized water. The absorbance at 510 nm was measured by UV/vis spectrophotometer.

Determination of molar absorption coefficient of $K_3Fe(C_2O_4)_3$ (ε_{365}). Take 0.5, 1.0, 1.5, 2, 2.5, 3 and 3.5 mL of 4.079×10^{-3} mol/L $K_3Fe(C_2O_4)_3$, into volumetric flasks respectively, and then dilute to 10.0 mL with deionized water. The absorbance at 365 nm was measured by UV/Vis spectrophotometer.

Determination of molar absorption coefficient of stearic acid (ε_{410}). Since stearic acid has no absorption at the wavelength of 410 nm, the molar absorption coefficient of the reagent used in the reaction is selected as the molar absorption coefficient of the whole reaction solution. TiO_2 concentrations were prepared as 0.625×10^{-3}, 1.25×10^{-3}, 1.875×10^{-3}, 2.5×10^{-3}, 3.75×10^{-3} mol/L n-tetradecane suspension respectively. The absorbance at 410 nm was measured by UV/vis spectrophotometer.

Determination of the effective optical path of the quartz reactor. Take 1, 2, 3, 4 and 5 mL of 6.119×10^3 mol/L $K_3Fe(C_2O_4)_3$, into 25 mL volumetric flasks respectively, and dilute to scale with distilled water. Then the above solution was added to a quartz reactor and was irradiated by LED (410 nm, 10.25 W/cm^2) with continuous stirring (300 r.p.m) and continuous water cooling for 5 min, respectively. Meanwhile, take 5 mL of the above reaction solution, 2.5 mL of 0.1% aqueous 1,10-phenanthroline solution, and 6.25 mL buffer solution into 50 mL brown volumetric flasks, and adjust with distilled water. The absorbance at 510 nm was measured by UV/vis spectrophotometer.

The AQE of fatty acids under LED (410 nm, 10.25 W/cm^2) illumination. Determination of molar absorptivity: The absorbance values of Fe^{2+}, $K_3Fe(C_2O_4)_3$ and stearic acid measured by spectrophotometer were regressed to get the equation, and the slope was the molar absorption coefficient. The regression equation of Fe^{2+} is Y=9204X-0.01 (R^2=0.9985), so the molar absorption coefficient of Fe^{2+} is 9.204×10^3 $(mol/L)^{-1} \cdot cm^{-1}$. The regression equation of $K_3Fe(C_2O_4)_3$ is Y=653.47X-0.0144 (R^2=0.9997), so the molar absorption coefficient of $K_3Fe(C_2O_4)_3$ is 653.47 $(mol/L)^{-1} \cdot cm^{-1}$. Because stearic acid has no absorption at the wavelength of 410 nm, the molar absorption coefficient of TiO_2 at 410 nm was selected as the molar absorption coefficient of the whole reaction solution in this experiment, and the equation is Y=515.46X+0.9000 (R^2=0.8985). Therefore, the molar absorption coefficient of stearic acid is 515.46 $(mol/L)^{-1} \cdot cm^{-1}$.

The effective optical path for a quartz reactor can be calculated by the following equation:

$$-\frac{dc}{dt} = R_c = fI_{0\lambda}V(1-10^{-\varepsilon cL})$$

(S5)

When $\varepsilon cL > 2.0$, the maximum rate was calculated as follows:

$$R_{max} = \Phi I_{0\lambda}V$$

(S6)

where ε is the molar absorption coefficient of the actinometer, c is the concentration of the actinometer, L is the effective optical path of the quartz reactor, $I_{0\lambda}$ is the incident light intensity and V is the constant related to the light container.

(S5) / (S6), that is,

$$\frac{R_c}{R_{max}} = 1-10^{-\varepsilon cL} = x$$

(S7)

which is:

$$-\lg(1-x) = \varepsilon cL$$

(S8)

The slope of the line of -lg(1-x) versus εc obtained by linear regression is the effective optical path of the quartz reactor. The effective optical path of the quartz reactor is 6.59 cm under LED (410 nm, 10.25W/cm^2) illumination.

The rate constant for the degradation reaction of $K_3Fe(C_2O_4)_3$ is 1.0×10^{-4} mol·L^{-1}·min^{-1} under LED (410 nm, 10.25 W/cm^2) illumination. The measured quantum efficiency can be obtained by substituting the measured data into Equation S4.

Photothermal conversion efficiency

The photothermal conversion efficiency was measured based on a reported work[3]. The photocatalytic decarboxylation reaction system was employed as a model to set the measurement parameters, i.e., n-tetradecane was used as the heating medium. The photothermal conversion efficiency η can be calculated by:

$$\eta=\frac{(T_{eq}-T_{am})nC_{p,liquid}B}{AS_m}$$

(S9)

Where T_{eq} is the equilibrium temperature for the n-tetradecane medium, 254 °C; T_{am} is ambient temperature, 22 °C; n is the amount of substance of the n-tetradecane, 0.09612 mol; $C_{p,\ liquid}$ is the constant pressure heat capacity of liquid n-tetradecane, 438.28 J·mol^{-1}·K^{-1}; B is the constant rate of heat dissipation, which can be determined from the Equation S9 (see Figure S2), 2.05×10^{-3} s^{-1}; A is the area exposed to irradiation, 50.24 cm^2; S_m is the incident irradiance of 410nm LED array, 10.25 W·cm^{-2}.

$$\frac{T(t)-T_{am}}{T_{eq}-T_{am}} = \exp(-Bt)$$

(S10)

Where $T(t)$ is the temperature at time t, °C, t is time after light off, s.

Catalyst stability experiments

Recycle test of the catalyst experiments conditions: The run was done under LED (10.25 W/cm^2, 410 nm) illumination for 0.5 h with fresh 0.1875 g of catalyst (1st use), 5 mmol of n-octadecane, 5 mmol of stearic acid and 21.8 mL n-tetradecane solvent. After the reaction finished, the catalysts were recovered by washing with methanol and drying at 80 °C for 5 h, then employed directly in a new run. Because of the strong adsorption capacity of the catalyst, it is easy to be adsorbed on the reactor, resulting in a small loss

of catalyst in the recovery process. The loading of the catalyst for the subsequent two runs was 0.1750 g (2nd use) and 0.1256 g (3rd use), respectively.

The long-term cycle experiments were completed using continuous addition of raw materials, avoiding loss of catalyst due to liquid-solid separation. The starting reaction solution includes n-tetradecane solvent(15 mL), stearic acid (1.25 mmol (= 0.05 M in 25 mL reaction solution)), n-octadecane (1.25 mmol), and TiO_2 (125 mg). The reaction temperature was locked by the n-tetradecane solvent at 254 °C. Each cycle was illuminated for 30 min (410 nm LED 10.25 W/cm^2) in a sealed batch photo-reactor with filled N_2. After completing one cycle, the photo-reactor was unsealed and 0.5 mL of the sample was taken for quantitative analysis. Before starting the next cycle, equal mmol of stearic acid (1.25 mmol, 0.3554 g) and n-octadecane (1.25 mmol, 0.3181 g), respectively, were added to the batch photo-reactor again and the batch photo-reactor was resealed and refilled with N_2 to start the photocatalytic reaction. Follow this process each time, a total of 30 cycles.

Theoretical calculation

First-principles calculations were used to get the stable TiO_2 catalyst configuration. It was carried out on the basis of periodic DFT using a generalized gradient approximation within the Perdew-Burke-Ernzerh of exchange correction functional within the Vienna Ab initio Simulation Package (VASP). The geometry optimization was first conducted with Gamma centered k-point with 3×3×1 mesh. The wave functions were constructed from the expansion of plane waves with an energy cutoff of 450 eV. The consistency tolerances for the geometry optimization were set as 1.0×10^{-5} eV/atom for total energy and 0.05 eV/Å for force, respectively. Before molecular dynamic (MD) simulation, the TiO_2 slab was expanded to a large supercell to avoid the interaction between adsorbed stearic acid in adjacent cells. Then, adsorbed stearic acid was established on the TiO_2 slab with periodic boundary conditions, including 330 Ti and 660 O atoms in a box of 32 × 32 × 50 Å. A large vacuum layer of 20 Å was used to avoid the interaction between the two surfaces. MD simulations were performed to search the stable configuration under different temperatures. The ReaxFF force field was used to simulate the adsorption process. MD simulations were carried out in a Large-scale Atomic/Molecular Massively Parallel Simulator (LAMMPS) with a time step of 1.0 fs. The system was first equilibrated for 0.1 ns in an isothermal−isobaric (NVT) ensemble at a low temperature and zero pressure, ensuring the minimum energy and internal stress. Finally, the system temperature was raised up to the desired 35 and 250 °C. After 100 ps MD simulation, the system's total energy could reach the equilibrium state. The bond energy was calculated through the energy change between the original molecular and dissociation groups without any interaction.

Sunlight collection device

The sunlight collection device is mainly composed of a dish reflector system and an automatic sun tracking system, which controls the motor to adjust the angle of the reflector system in real time to focus the sunlight on the designated position. The power of the solar-focused spot is related to the spot diameter and collecting mirror area, and the relationship is shown in Equation S11.

$$P_{Focused} = \frac{P_{Sunlight} \times S_{Collected} \times R}{S_{Foused}}$$

(S11)

Where $P_{Focused}$ is the intensity of focused sunlight, W/m^2; $P_{Sunlight}$ is the intensity of natural sunlight, W/m^2, the average power is 1000 W/m^2; $S_{Collected}$ is the collecting mirror area, m^2, R is the reflection coefficient of the collecting mirror, 0.85; $S_{Focused}$ is the area of focused sunlight, m^2.

The scaled-up test conditions for 500 mL: the reaction solution (500 mL) involving TiO_2 (2.5 g), stearic acid (0.05 M), n-octadecane (0.05 M) and n-tetradecane solvent, collecting mirror area is 3.3 m² (focused sunlight intensity ~21 W/cm²), irradiation for 120 min, the air was pumped out of the reactor before the reaction. The top of the reactor is equipped with an air-cooled return pipe. The test was performed under solar radiation in Baotou, China (11/6/2017, 14 ~ 30 °C).

The scaled-up test conditions for 1500 mL: the reaction solution (1500 mL) involving TiO_2 (7.5 g), stearic acid (0.1 M) and n-tetradecane as the solvent, collecting mirror area is 9.5 m² (focused sunlight maximum intensity ~26 W/cm²). The air was pumped out of the reactor before the reaction. The top of the reactor is equipped with an air-cooled return pipe. The test was performed under solar radiation in Baotou, China (29/6/2023, 14 ~ 35 °C and 30/6/2023, 16 ~ 36 °C).

The solvent and product were separated by reduced pressure distillation and the *isolated yield* was calculated as follows:

$$Isolated\ Yield = \frac{Actual\ yield\ \text{(mL)}}{Theoretical\ yield\ \text{(mL)}} \times 100\% \tag{S12}$$

The theoretical yield of n-heptadecane product from the scale-up test of 1500 mL was 46.4 mL after >99% conversion of stearic acid, and a 36.6 mL actual yield was obtained by reduced pressure distillation.
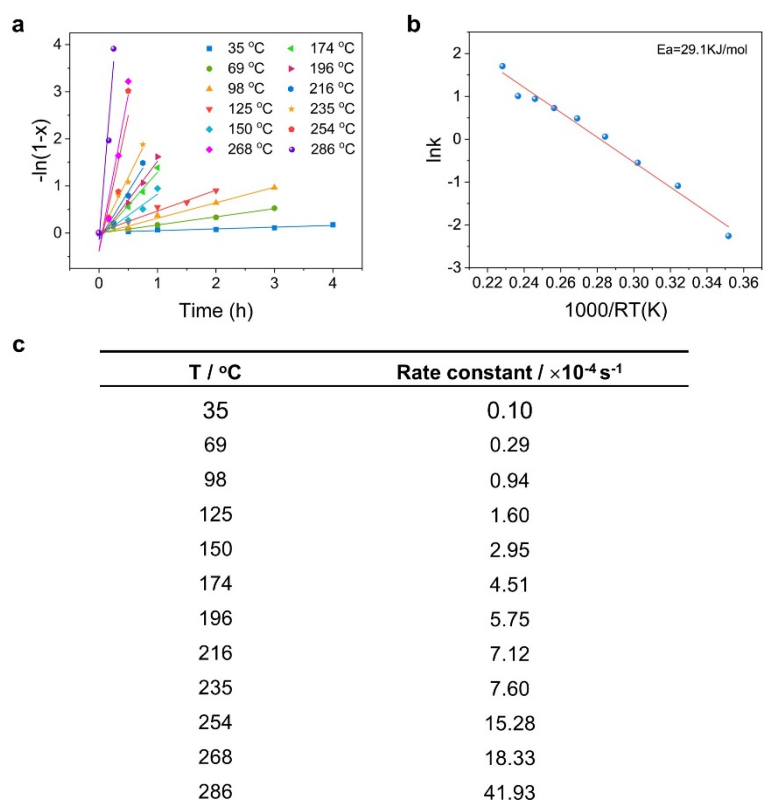
Results and discussion
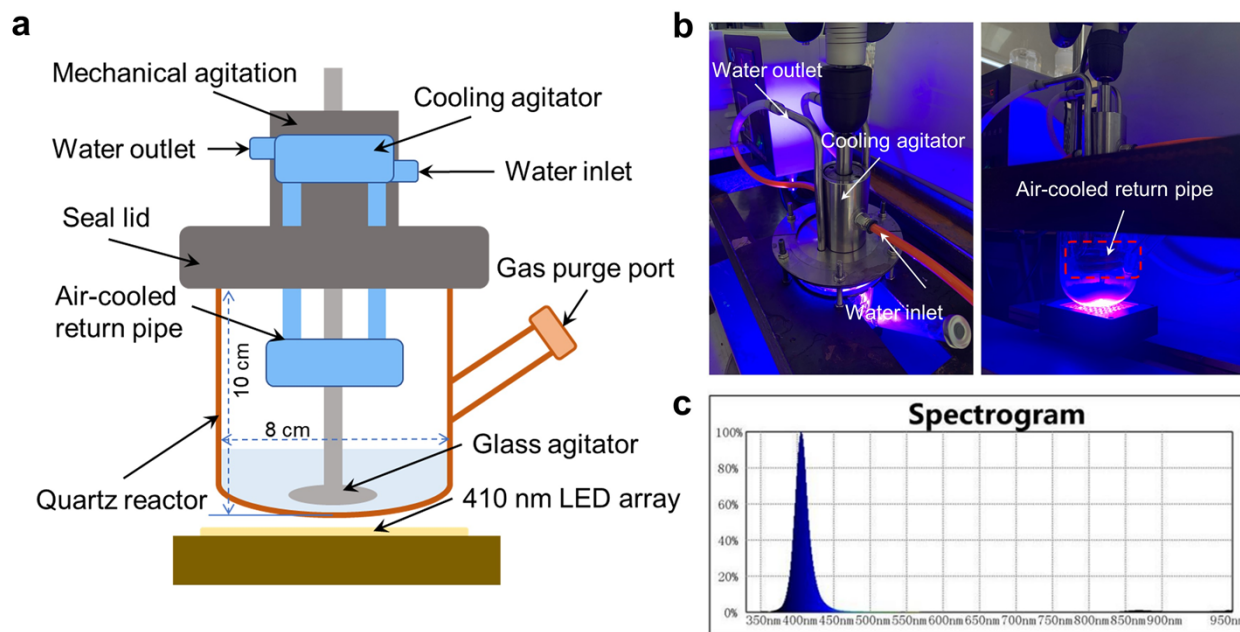
Figure S1. Self-heating photocatalytic reaction system. (a) Schematic illustration of self-heating photocatalytic reaction system. (b) Self-heating photocatalytic reaction system. (c) The wavelength distribution of 410 nm LED array in the system.
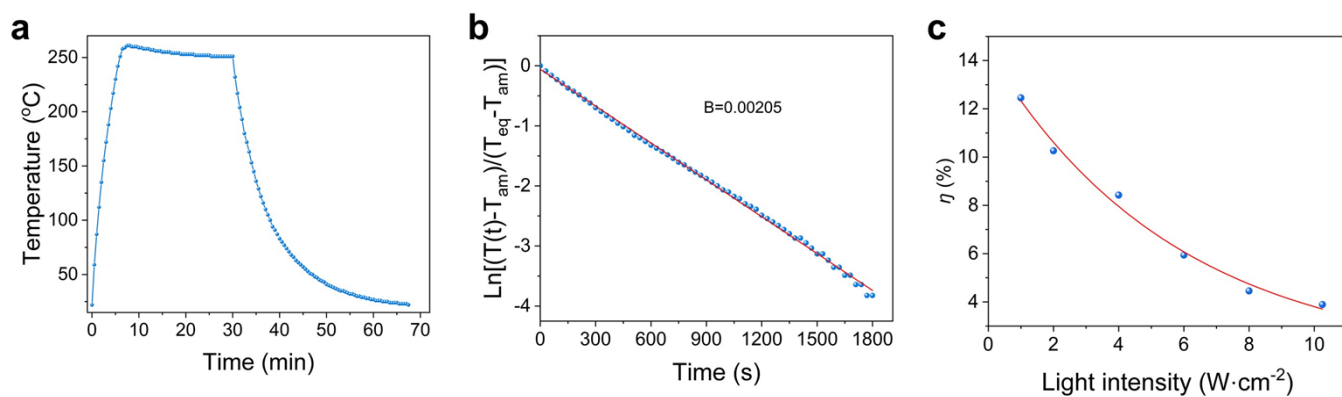
Figure S2. Determination of heat dissipation coefficient of the reaction system. (a) Real-time monitoring of temperature rise of reaction solution under 410 nm LED illumination (10.25W/cm^2). (b) Plotting natural log of $(T(t) - T_{am}) / (T_{eq} - T_{am})$ versus time t after the 410 nm LED (10.25 W/cm^2) was turned off. (c) Light intensity dependence of photothermal conversion efficiency η of TiO_2 under 410 nm LED illumination. Condition: TiO_2 (125 mg), n-tetradecane (25 mL), N_2 atmosphere.
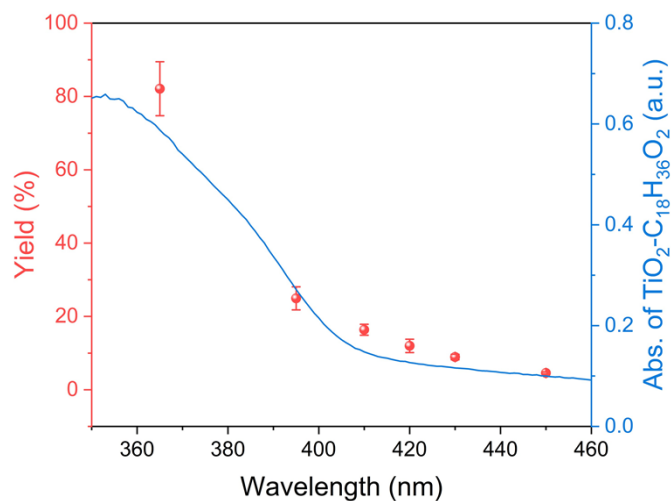
Figure S3. Wavelength dependence of photocatalytic stearic acid decarboxylation. Reaction conditions: reaction solution volume (25 mL), TiO$_2$ (125 mg), stearic acid (0.05 M), n-octadecane (internal standard, 0.05 M), reaction pressure (0.1 MPa), external heat to the boiling point of n-tetradecane (254 °C) (Since the self-heating effect of TiO$_2$ decreases with increasing wavelength, external heat supply was used to ensure a constant temperature.), N$_2$ atmosphere, LED (1.65 W/cm^2) irradiation for 20 min. The yield of n-heptadecane was determined by gas chromatography analysis. All catalytic performance data in the graphs are averages of at least three experiments.

a

■ 35 °C	◀ 174 °C
● 69 °C	▶ 196 °C
▲ 98 °C	● 216 °C
▼ 125 °C	★ 235 °C
◆ 150 °C	● 254 °C
◆ 268 °C	● 286 °C

b Ea=29.1KJ/mol

c

T / °C	Rate constant / ×10⁻⁴ s⁻¹
35	0.10
69	0.29
98	0.94
125	1.60
150	2.95
174	4.51
196	5.75
216	7.12
235	7.60
254	15.28
268	18.33
286	41.93

Figure S4. Kinetics of photocatalytic decarboxylation of stearic acid over TiO_2. (a) -ln(1-x) vs. time plots of stearic acid photocatalytic decarboxylation at different n-alkane boiling point temperatures and 35 °C (C6 ~ C14, 69 ~ 254 °C). x= yield of n-heptadecane. (b) Arrhenius plots for the photocatalytic stearic acid decarboxylation. (c) Photocatalytic stearic acid decarboxylation rate constant (s⁻¹) at different temperatures over TiO_2.
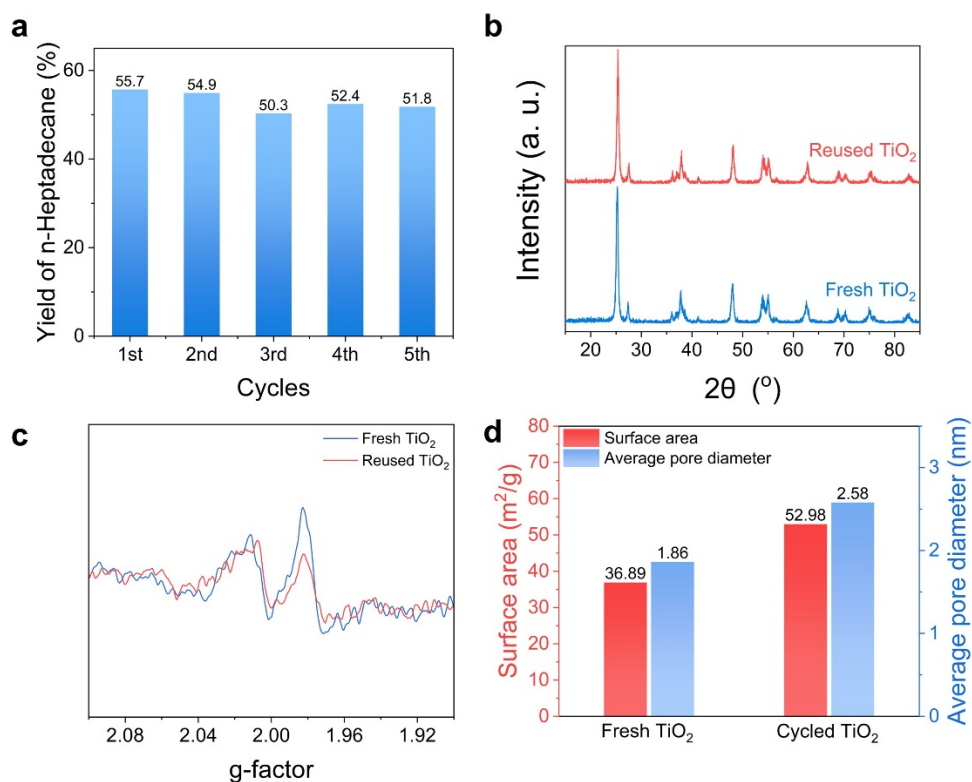
Figure S5. Stability of TiO_2 catalyst. (a) Recyclability in photocatalytic stearic acid decarboxylation over TiO_2. (b) XRD spectrum of fresh and reused TiO_2 catalyst after fifth catalytic cycles. (c) The ESR spectra of TiO_2 before and after the catalytic cycle. (d) BET surface area of fresh and reused TiO_2 catalyst after fifth catalytic cycles. Conditions: reaction solution volume (25 mL), stearic acid (0.2 M), TiO_2 (125 mg), n-octadecane (internal standard, 0.2 M), n-tetradecane solvent, LED (410 nm, 10.25 W/cm²) irradiation for 1.5 h.
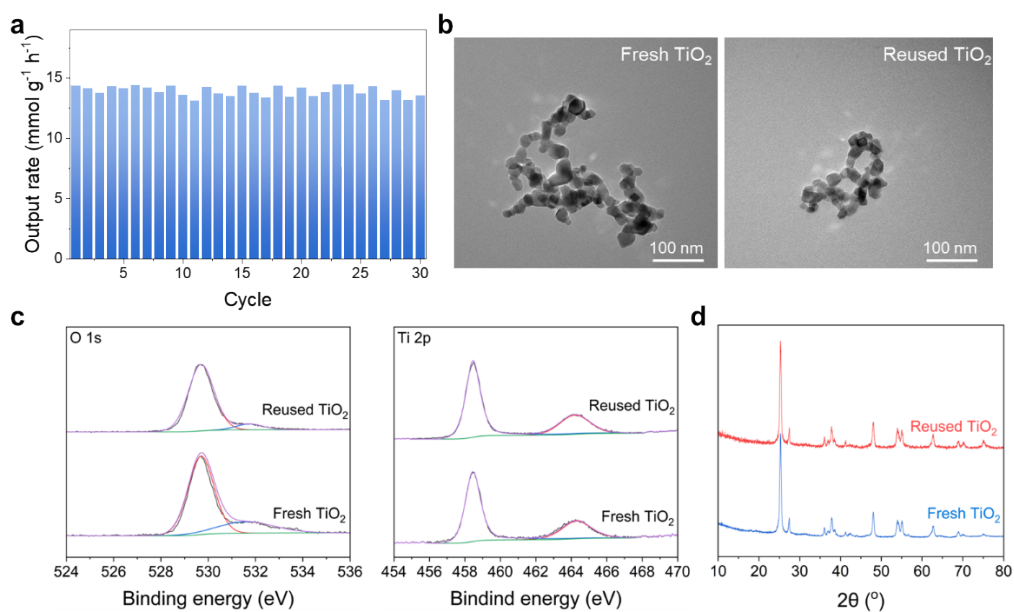
Figure S6. Multiple cycle stability of TiO$_2$ catalyst. (a) Cycling tests of n-heptadecane output TiO$_2$ for 30 cycles. (b) The TEM analysis of TiO$_2$ before and after the catalytic cycle. (d) XPS spectrum of fresh and reused TiO$_2$ catalyst after 30 catalytic cycles. (d) XRD spectrum of fresh and reused TiO$_2$ catalyst after 30 catalytic cycles. Conditions: n-tetradecane (15 mL), stearic acid (1.25 mmol), TiO$_2$ (125 mg), n-octadecane (internal standard, 1.25 mmol) in first cycle; LED (410 nm, 10.25 W/cm^2) irradiation for 30 min in every cycle; add stearic acid (1.25 mmol) and n-octadecane (1.25 mmol) in every cycle.

a CH₃-(CH₂)₁₅-CH₃
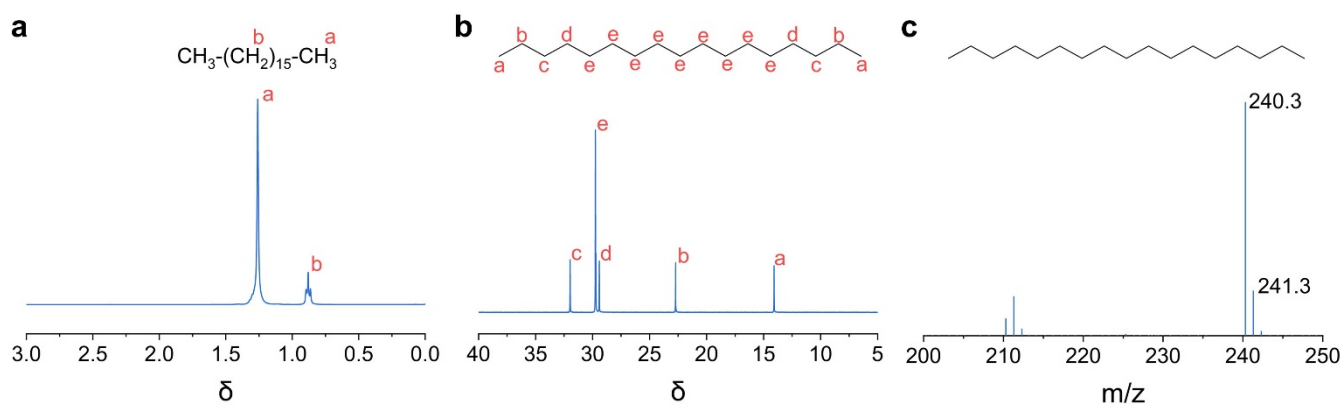
Figure S7. The analysis of the isolated product of the scaled-up reaction. (a) ^{1}H-NMR spectra of the isolated product. (b) ^{13}C-NMR spectra of the isolated product. (c) Mass spectra of the isolated product.
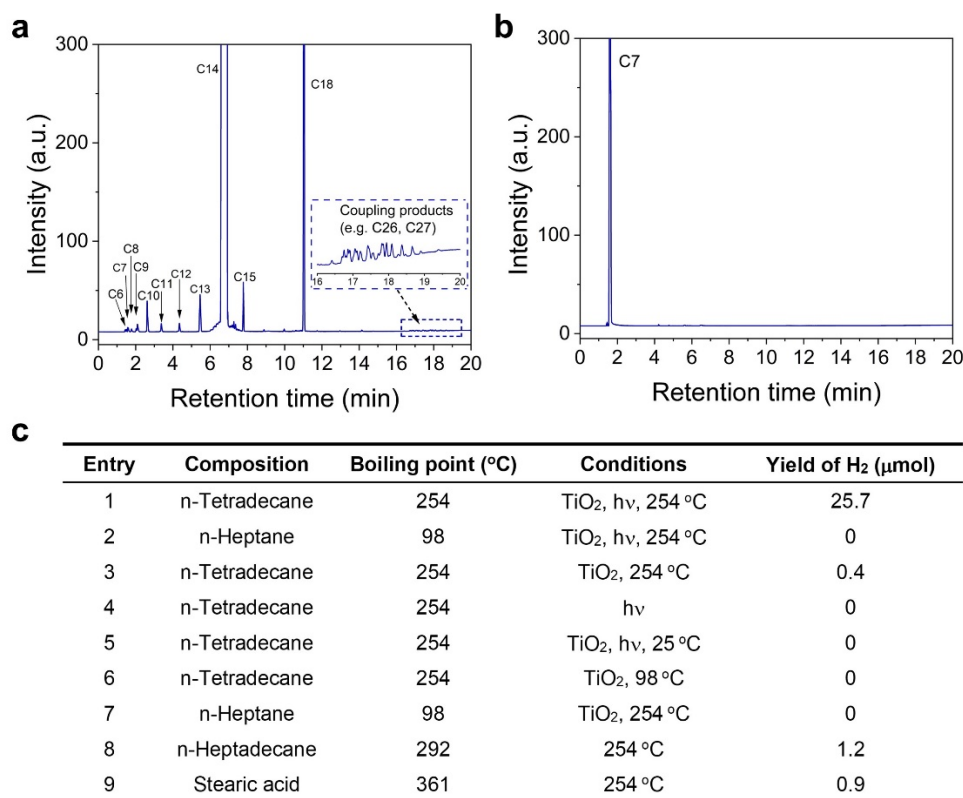
Figure S8. The product distribution analysis. (a) The gas chromatogram of photocatalytic n-tetradecane solvent over TiO_2. (b) The gas chromatogram of photocatalytic n-heptane solvent over TiO_2. Reaction conditions: the total volume of the reaction solution was 25 mL. N_2 atmosphere, ambient pressure, n-octadecane (internal standard, 0.05 M), n-tetradecane (solvent), TiO_2 (125 mg), visible light (410 nm LED, 10.25 W/cm^2) irradiation with no external heating, irradiation for 0.5 h. (c) ^{1}H-NMR spectra of n-heptadecane product. (c) ^{13}C-NMR spectra of n-heptadecane product. (e) High-temperature dehydrogenation of the reaction solution. General condition: a single component of the reaction solution was subjected to a comparison of conditions to examine the dehydrogenation of the reaction solution at high temperatures. The composition volume (25 mL), 0.5 h, N_2 atmosphere.

The n-tetradecane contains traces of carbon products (n-tridecane and n-pentadecane are impurities of commercialized n-tetradecane and n-octadecane is an internal standard) as well as coupling products under the photothermal heat of TiO_2, while heptane was not detected, suggesting that the high temperatures caused a slight dehydrogenation of the alkanes, which, however, had a negligible effect on the decarboxylation reaction.
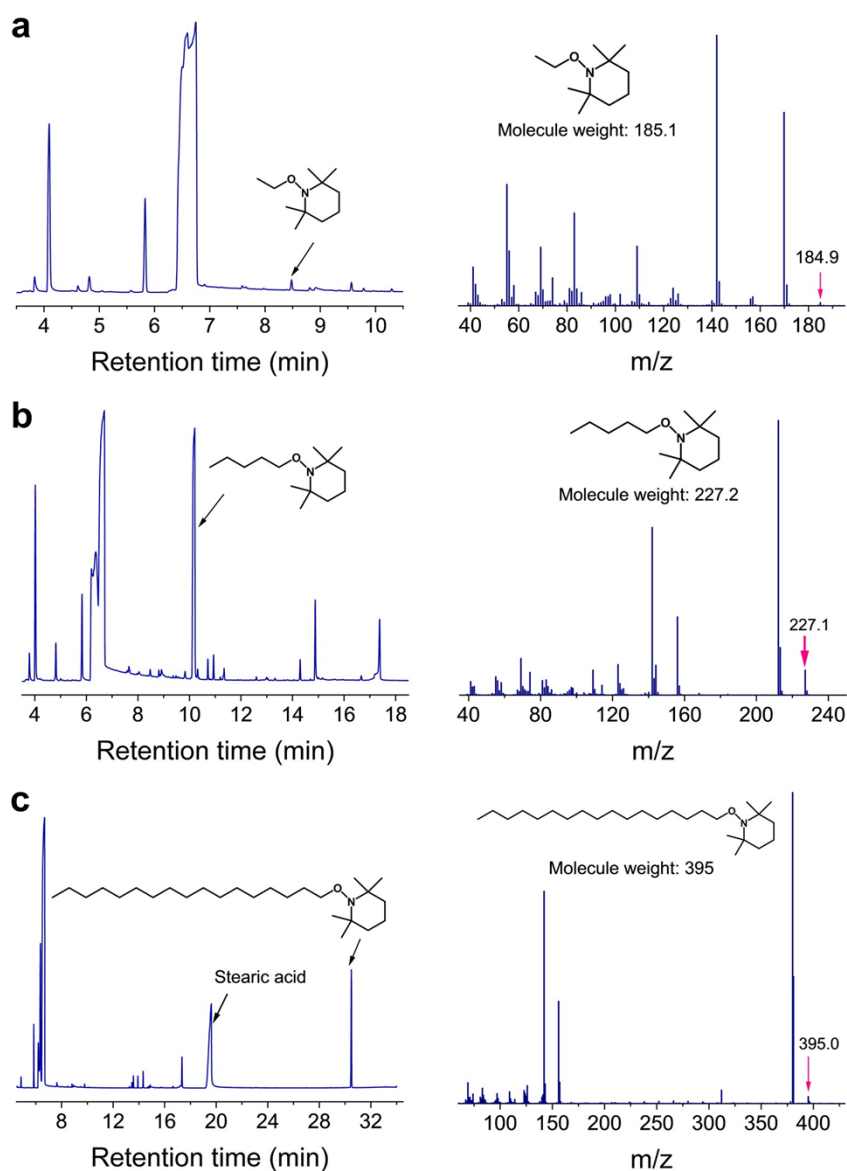
Figure S9. Radical capture experiments. (a) GC-MS analysis of the propionic acid decarboxylation reaction solution after incorporation of TEMPO. (b) GC-MS analysis of the hexanoic acid decarboxylation reaction solution after incorporation of TEMPO. (c) GC-MS analysis of the stearic acid decarboxylation reaction solution after incorporation of TEMPO. General reaction condition: fatty acid (0.05 M), TEMPO (0.3 M), TiO_2 (125 mg), n-hexane solvent (24 mL), LED (410 nm, 10.25 W/cm^2) irradiation for 1.5 h.

To investigate whether this photocatalytic decarboxylation reaction contains free radical intermediates, TEMPO was added to the system to trace the free radicals. The products of TEMPO after trapping the alkyl radicals were found to confirm the presence of free radicals during the photocatalytic decarboxylation reaction.
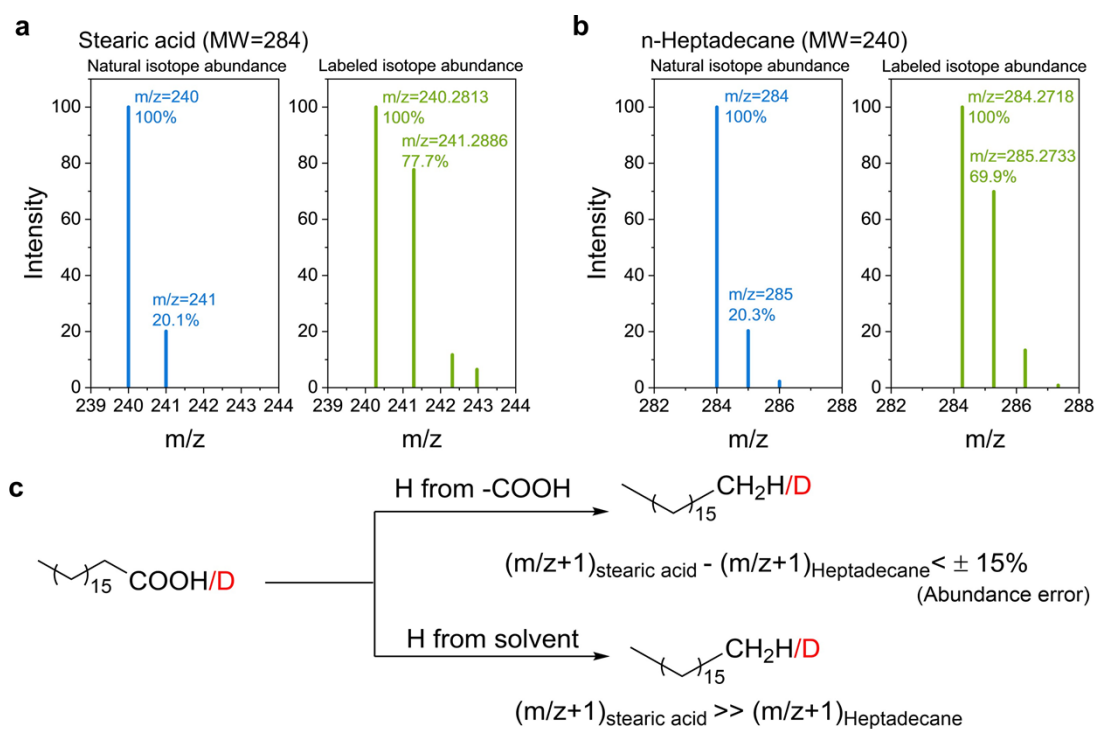
Figure S10. Hydrogen source for n-heptadecane in the photocatalytic decarboxylation of stearic acid. (a) Mass spectra of natural stearic acid (from the NIST database) and mass spectra of isotope-labeled carboxyl hydrogen stearic acid. (b) Mass spectra of natural n-heptadecane (from NIST database) and mass spectra of n-heptadecane from labeled stearic acid decarboxylation. (c) Possible reaction pathways for photocatalytic decarboxylation of isotope-labeled stearic acid.

Figure S8 clarifies the source of hydrogen for the formation of products in the decarboxylation reaction. It is difficult to prepare high-purity $C_{17}H_{35}COOD$ due to the more reactive hydrogen of the carboxyl group, which makes it easy to exchange hydrogen with water in the air, and there is still a large amount of $C_{17}H_{35}COOH$. The natural abundance of m/z+1 for both stearic acid and n-heptadecane was about 20%, and the abundance of m/z+1 for labeled stearic acid increased significantly, indicating that some of the carboxyl hydrogens were deuterated. The abundance of m/z+1 in the n-heptadecane prepared from this stearic acid was basically the same as that of the feedstock stearic acid, and the deviation was within the error of mass spectrometry analysis, indicating that the hydrogen source for n-heptadecane is mainly carboxyl hydrogen, otherwise, the abundance of m/z+1 would be considerably lower.
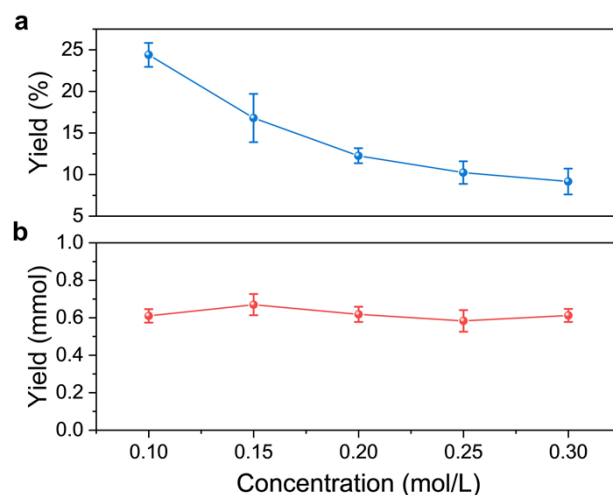
Figure S11. Concentration expansion of the photocatalytic decarboxylation reaction of stearic acid over TiO_2. (a) The percentage yield of stearic acid decarboxylation concentration expansion. (b) The absolute yield of stearic acid decarboxylation concentration expansion. Reaction conditions: reaction solution volume (25 mL), TiO_2 (125 mg), stearic acid, n-octadecane (internal standard, 0.05 M), reaction pressure (0.1 MPa), n-tetradecane solvent locked reaction temperature (254 °C), LED (410 nm, 10.25 W/cm^2) irradiation for 30 min. All catalytic performance data in the figure are averages of at least three experiments.

The increasing initial concentration resulted in a decrease in the percentage yield (Figure S9a), while the absolute yield basically stabilized at about 0.6 mmol (Figure S9b), indicating that it was saturated with stearic acid adsorption and the rate of photocatalytic conversion was limited by the number of active sites in the catalyst.
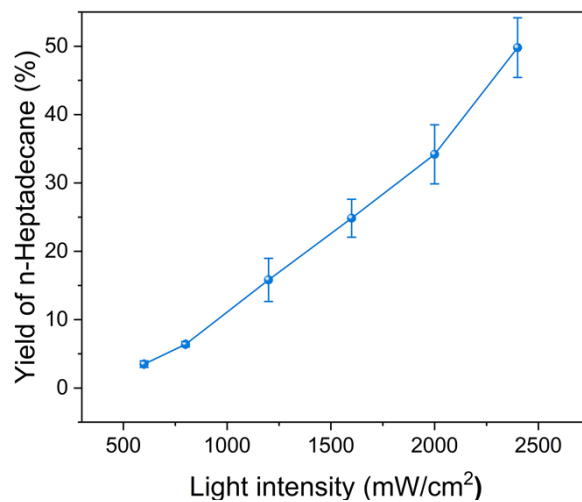
Figure S12. Variation of n-heptadecane yield with light intensity. Reaction conditions: reaction solution volume (5 mL), TiO$_2$ (25 mg), stearic acid (0.05 M), n-octadecane (internal standard, 0.05 M), reaction pressure (0.1 MPa), n-decane solvent locked reaction temperature (174 °C), Xenon lamp irradiation for 2 h. All catalytic performance data in the figure are averages of at least three experiments.
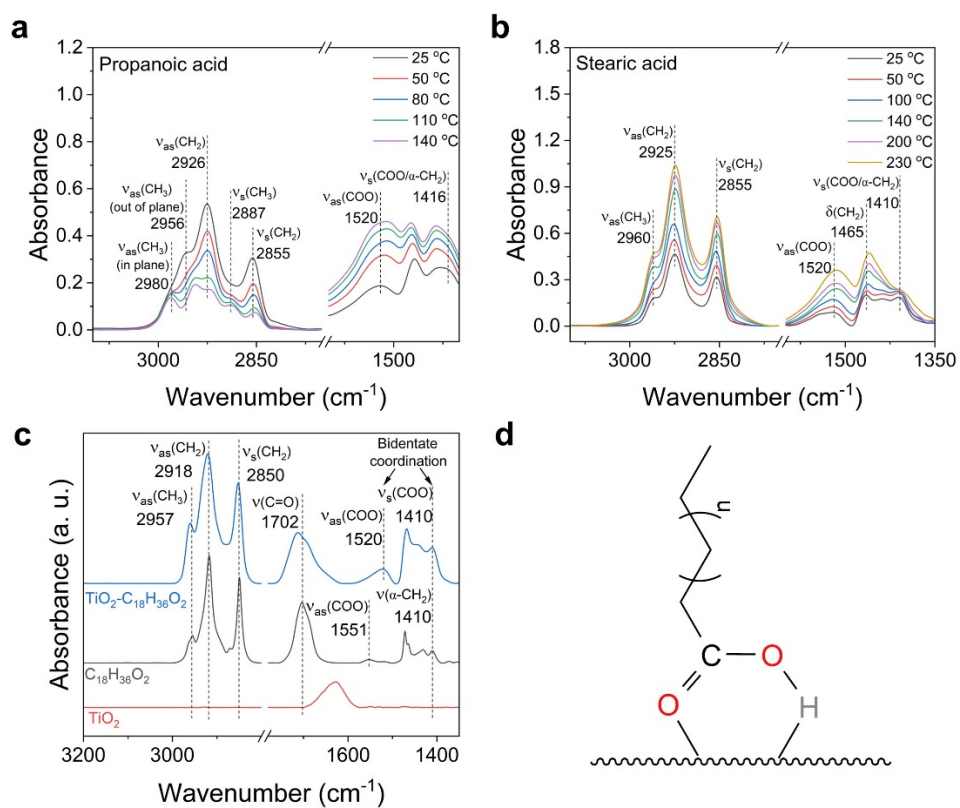
Figure S13. In situ DRIFT spectra. (a) In situ DRIFT spectra of propionic acid over TiO_2 with programmed temperature process (25 ~ 140 ºC). (b) In situ DRIFT spectra of stearic acid over TiO_2 with programmed temperature process (25 ~ 230 ºC). (c) Diffuse reflectance FTIR spectroscopy of dissolved and adsorbed stearic acid on TiO_2, respectively, at room temperature and the schematic (d)
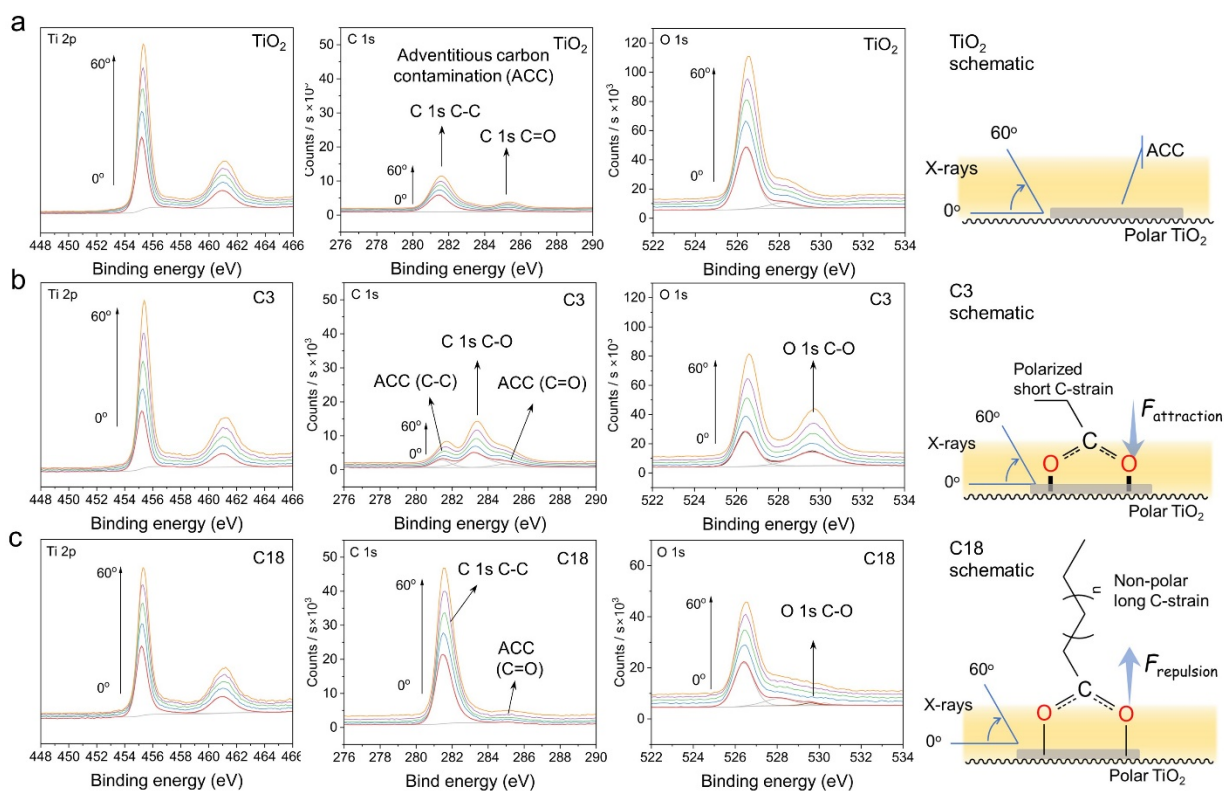
Figure S14. Room-temperature angle-resolved XPS and schematic of propionic acid and stearic acid over TiO_2 (angular scanning range: 0~60°). (a) TiO_2. (b) Propionic acid loaded on TiO_2. (c) Stearic acid loaded on TiO_2. TiO_2 powder adsorbed with 20 wt% fatty acids or TiO_2 powder was pressed into sheets of about 1 mm thickness.
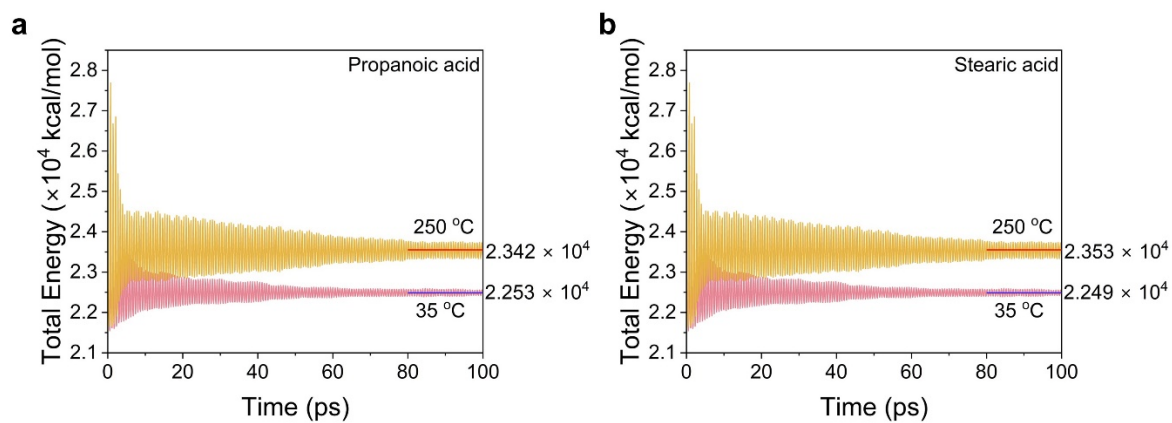
Figure S15. Relative energies of propionic acid (a) and stearic acid (b) models reaching steady state after molecular dynamics simulation at different temperatures.
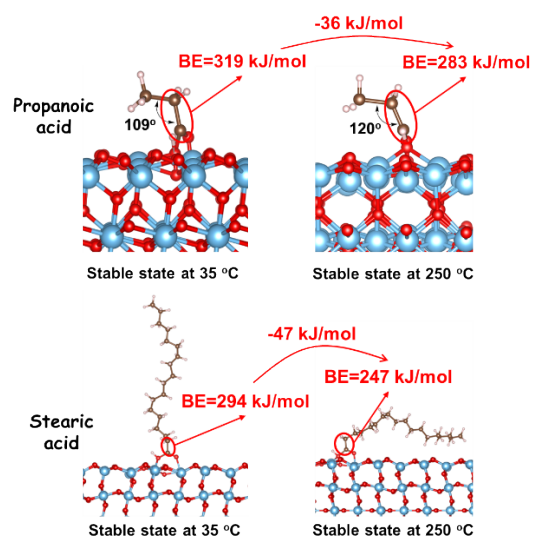
Figure S16. α-C-COO bond energies (BE) of the conformations of propionic acid and stearic acid at different temperatures.

Table S1. Comparison of fatty acid conversion between previous works and the current study

Catalyst	Substrate concentration (mol/L)	Solvent	Reaction conditions	Conv. (%)	C_{n-1} Alkane Yield (%)	Average production rate (mmol g^{-1} h^{-1}) [a]	Ref.
20% Ni/C	Lauric acid (0.120)	Water	350 °C, 4 h	79.1	70	1.17	4
Activated carbon	Palmitic acid (0.271)	Water	370 °C, 3 h	33	19	0.82	5
1.19 w% Pt/NMC	Stearic acid (0.000176)	Tetradecane	330 °C, 3 h	100	97.2	3.91	6
5 wt% Pd/C	Stearic acid (0.138)	Dodecane	300 °C, He 0.6 MPa, 6 h	100	95	2.50	7
10 wt% Ni/ZrO$_2$	Stearic acid (0.035)	Dodecane	260 °C, H$_2$ 4 MPa, 8 h	100	96	0.89	8
Ni/zeolite	Stearic acid (0.035)	Dodecane	260 °C, H$_2$ 4 MPa, 8 h	100	14.8	0.32	9
[Ni] catalyst	Palmitic acid (0.0001)	THF	40 °C, 12 h	-	51	0.77	10
1 wt% NM/TiO$_2$	Lactic acid (0.5)	Water	20 °C, 3 h, 500 W Hg (Xe)	9.5	3.4	5.67	11
1 wt% Pt/TiO$_2$	Stearic acid (0.033)	Acetonitrile	30 °C, H$_2$ 0.1 MPa, UV-LED irradiation, 2 h	96	92	2.30	12
1 wt% Pt/TiO$_2$	Lauric acid (0.050)	Acetonitrile	30 °C, H$_2$ 0.1 MPa, UV-LED irradiation, 2 h	>99	93	3.49	12
TiO$_2$	Stearic acid (0.5)	n-Tetradecane	410 nm LED irradiation (10.25 W/cm^2), 6 h	100	86.2	14.37	This work
TiO$_2$	Palmitic acid (0.05)	n-Heptadecane	410 nm LED irradiation (10.25 W/cm^2), 0.5 h	100	84.5	33.8	This work
TiO$_2$	Stearic acid (0.05)	n-Hexadecane	410 nm LED irradiation (10.25 W/cm^2), 0.5 h	100	98.2	40.73	This work
TiO$_2$	Lauric acid (0.05)	n-Heptadecane	410 nm LED irradiation (10.25 W/cm^2), 0.5 h	100	72.3	28.92	This work

[a] The calculation of the average reaction rate is based on the yield of C_{n-1} n-alkane.

Movie S1. The scaled-up test under focused sunlight for 500 mL. Up-scaled reaction with volumes of 500 mL. The starting concentration of stearic acid was 0.05 M. The collecting mirror area of the dish-shaped concentrator is 3.3 m², and the intensity of the focused sunlight is 21 W/cm². The air was pumped from the system before the reaction. The top of the reactor was equipped with a recirculating cooling water system to reflux the reaction solution. The reaction solution under an intense boiling state allowed the stirring to be optional. The test was performed under solar radiation in Baotou, China (11/6/2017, 14-30 °C).

Movie S2. The scaled-up test under focused sunlight for 1500 mL. Up-scaled reaction with volumes of 500 mL. The starting concentration of stearic acid was 0.1 M. The collecting mirror area is 9.5 m², and the intensity is 26 W/cm². The top of the reactor was equipped with a recirculating cooling water system to reflux the reaction solution. The air was pumped from the system before the reaction. The test was performed under solar radiation in Baotou, China (29/6/2023, 14 ~ 35 °C and 30/6/2023, 16 ~ 36 °C).

Movie S3. The MD movies of the fatty acid models at different temperatures.

References

1. Z. Ping, L. I. U. Zhengwen, L. I. N. Zhifen and K. Linren, *J. Jinan Univ.*, 2006, **27**, 465-469.
2. C. G. Hatchard and C. A. Parker, *Proc. Math. Phys. Eng. Sci*, 1956, **235**, 518-536.
3. L. L. Wang, M. Wang, Z. P. Xu, W. Yu and H. Q. Xie, *Sol. Energ. Mat. Sol. C.*, 2020, **212**, 110575.
4. J. H. Wu, J. J. Shi, J. Fu, J. A. Leidl, Z. Y. Hou and X. Y. Lu, *Sci. Rep.*, 2016, **6**.
5. J. Fu, F. Shi, L. T. Thompson, X. Y. Lu and P. E. Savage, *ACS Catal.*, 2011, **1**, 227-231.
6. Y. X. Liu, X. J. Yang, H. Y. Liu, Y. H. Ye and Z. J. Wei, *Appl. Catal. B Environ.*, 2017, **218**, 679-689.
7. M. Snare, I. Kubickova, P. Maki-Arvela, K. Eranen and D. Y. Murzin, *Ind. Eng. Chem. Res.*, 2006, **45**, 5708-5715.
8. B. X. Peng, X. G. Yuan, C. Zhao and J. A. Lercher, *J. Am. Chem. Soc.*, 2012, **134**, 9400-9405.
9. B. X. Peng, Y. Yao, C. Zhao and J. A. Lercher, *Angew. Chem. Int. Ed.*, 2012, **51**, 2072-2075.
10. M. D. B. da Silva, J. G. L. de Araujo, J. Bento, A. M. de Azevedo, C. R. O. Souto, A. S. D. dos Anjos, A. M. M. de Araujo, D. R. da Silva, F. G. Menezes, A. D. Gondim and L. N. Cavalcanti, *RSC Adv.*, 2022, **12**, 27889-27894.
11. K. T. Liu, A. Litke, Y. Q. Su, B. G. van Campenhout, E. A. Pidko and E. J. M. Hensen, *Chem. Commun.*, 2016, **52**, 11634-11637.
12. Z. P. Huang, Z. T. Zhao, C. F. Zhang, J. M. Lu, H. F. Liu, N. C. Luo, J. Zhang and F. Wang, *Nat. Catal.*, 2020, **3**, 170-178.